Dominant Screening Process in the Projectile Electron Loss for F⁻ + Ar Collisions

M. M. Sant'Anna

Instituto de Física, Universidade Federal do Rio de Janeiro, Cx. Postal 68528, Rio de Janeiro 21941-972, Brazil

A comparison between projectile electron loss cross sections for negative, F⁻, and positive, He⁺, projectiles is presented for collisions with Ar target. The behavior of the two collision systems is similar for the projectile electron loss with target ionization. For projectile electron loss without target ionization (the so-called *screening* electron-loss process), quite different situations are presented for the studied positive and negative projectiles. For He⁺ + Ar, the loss without target ionization collision channel is negligible for intermediate-to-low energies. On the other hand, for F⁻ + Ar, this collision channel is the dominant one in the total projectile electron loss at intermediate-to-low velocities. The roles played by coupling with the electron capture by the projectile collision channel and by the very different binding energies for negative and positive projectiles are discussed.

Keywords: Anion; Negative ions; Collision; Projectile electron loss

I. INTRODUCTION

Collisions between many-electron ionic projectiles and many-electron targets often occur in nature. Cross sections for these collisions are important parameters in the modeling of technological applications. However, a rigorous theoretical description of the multiple-ionization collision channels is a difficult task [1]. The experimental cross section data available are still scarce especially for anionic projectiles [2, 3]. Regarding projectile electron-loss the identification of two dynamically different collision processes, often called *screening* and *antiscreening* processes [4, 5], sheds light on the problem of the physical description of the collisions.

The beam-attenuation experimental technique allows the determination of the total projectile destruction cross section [6–8]. This cross section corresponds to the sum of single and all multiple projectile-electron-loss collision channels, regardless of the target final charge state. The collision channel for which the projectile loses one or more electrons and the target remains in the ground state is therefore included in those measurements. This latter collision channel is often called *screening* projectile electron loss (also called projectile elastic loss), since the field of the target nucleus, screened by their electrons, ionizes the projectile with no target excitation or ionization [4, 5].

Projectile electron loss also takes place with markedly different dynamics, in the so-called *antiscreening* process (sometimes named *two-center electron-electron correlation* process). Here the projectile-electron-target-electron interaction is responsible for the projectile electron loss. The target electron is the ionizing agent of the projectile and, due to the energy and momentum transfer to the projectile, has a high probability of being ionized simultaneously with the projectile electron. Thus, coincidence measurements for projectile and target final charge states can at least partially separate experimentally the *screening* and *antiscreening* processes specifying the cross sections $\sigma^{p,q}$ for the projectile (p) and target (q), final charge states [9, 10].

For positive ions there are at least two factors that complicate this experimental approach to the problem.

(i) The *screening* projectile electron-loss accompanied by the symmetrical process in the projectile frame of reference (namely the target direct ionization) produces the same final charge states as the *antiscreening* does. Experimental techniques like COLTRIMS can separate these collision channels (e.g. [11, 12]) but they will be undistinguishable in integrated cross sections obtained only by final charge-state coincidence measurements. The He⁺ + He and C³⁺ + Ne are examples of collision systems for which the simultaneous *screening* ionization of both target and projectile masks the *antiscreening* contribution to projectile electron loss. For He⁺ + He this is an important effect in the intermediate-to-low velocity range [9, 10]. For C³⁺ + Ne the effect is even stronger and the *antiscreening* contribution becomes negligible for low velocities [1].

(ii) The *antiscreening* process has an energy threshold similar to the one found in electron impact ionization [4, 5, 13]. The *screening* process is therefore, in principle, prominent below the *antiscreening* threshold. However, for low collision velocities electron capture by the projectile is very probable for positive ions and there is a strong coupling between the collision channels [1, 14, 15].

Anion projectiles offer a vast field to study the different dynamics of *screening* and *antiscreening* processes. This paper analyzes the F⁻ + Ar collision system in the intermediate velocity range, from 0.3 to 1.5 atomic units. For this collision system the *screening* contribution dominates the total projectile electron loss cross sections for intermediate-to-low velocities, in opposition to the case of positive projectiles illustrated by the He⁺ + Ar collision system. Possible effects of the absence of electron capture collision channel and of high asymmetry in projectile and target binding energies are discussed. Details on the experimental determination of F⁻ + Ar cross sections plus a comparison between F⁻ and other anionic projectiles, regarding projectile electron loss, will be presented in future work [16].

II.   *ANTISCREENING*: NEGATIVE VERSUS POSITIVE PROJECTILES

Figure 1 compares the projectile electron loss with target ionization for $F^- + Ar$ [16] and $He^+ + Ar$ [17, 18] collision systems. Cross sections are shown as a function of the projectile velocity divided by

$$v_{th} = \left((I_P + I_T) / Ry \right)^{1/2} v_0, \qquad (1)$$

where I_P and I_T are, respectively, the first projectile and target ionization potentials in Rydberg units (Ry), and v_0 is the Bohr velocity. The parameter v_{th} is a velocity characteristic of the *antiscreening* threshold and is equal to $1.19 \, v_0$ for $F^- + Ar$ and $2.27 \, v_0$ for $He^+ + Ar$. Cross sections are summed over contributions for final target charge states from 1 to 4.

Both data sets show the well known energy threshold for the *antiscreening* loss, although there may be contributions from the competing process for simultaneous projectile and target ejection discussed in the previous section. It is reasonable that the absolute values are higher for the F^- projectiles since it has more electrons than the He^+ projectile. The overall behavior is similar for the studied negative and positive projectiles in the overlapping v/v_{th} region of Fig. 1.

III.   *SCREENING*: NEGATIVE VERSUS POSITIVE PROJECTILES

Figure 2 shows projectile charge-changing cross sections for $He^+ + Ar$ collisions. The projectile electron loss without target ionization (circles), which contains the *screening* contribution, is small at low velocities. Actually, DuBois [14] estimated this contribution to be zero within the experimental errors of his measurements. An estimate for the upper bound of these uncertainties is represented by the dashed line in Fig. 2. DuBois made his estimate by subtracting from the total electron loss cross sections the partial cross sections for channels with charged final states. Thus corresponding uncertainty was obtained combining in quadrature estimated experimental errors in total electron loss cross sections and in *antiscreening* electron-loss cross sections. The *screening* contribution increases with velocity and is of the same order of magnitude of the *antiscreening* (squares) for the higher velocities represented in Fig. 2. Electron capture by the projectile (triangles) is by and large the dominant collision channel at low velocities but decreases very fast as the velocity increases and is irrelevant in the velocity range where *screening* and *antiscreening* are of the same order of magnitude ($v \approx 5v_0$ in Fig. 2).

Figure 3 compares $F^- + Ar$ projectile electron-loss cross sections (single + multiple) for collision channels with and without target ionization. The channel without target ionization corresponds to the *screening* mechanism (except for possible contributions from simultaneous projectile loss and target excitation, with posterior target fluorescent decay). This channel clearly dominates the total electron loss for intermediate-to-low velocities. The situation is opposite to
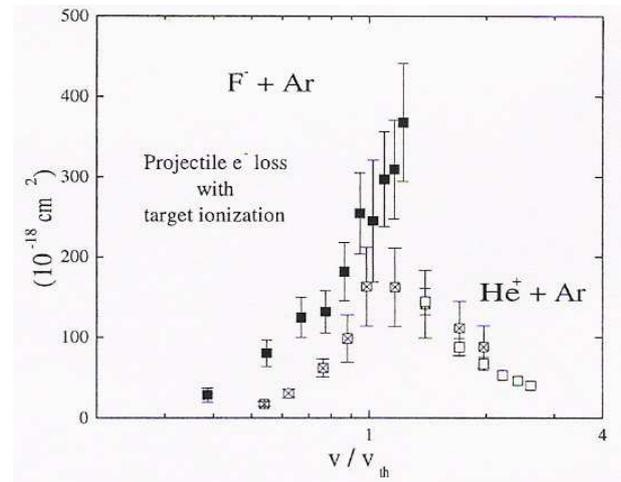

FIG. 1: Projectile electron-loss cross sections with target ionization (single + multiple) as a function of projectile velocity divided by v_{th} (see text). Solid symbols, $F^- + Ar$ [16]; x-center symbols, $He^+ + Ar$ [14]; open symbols, $He^+ + Ar$ [17, 18].
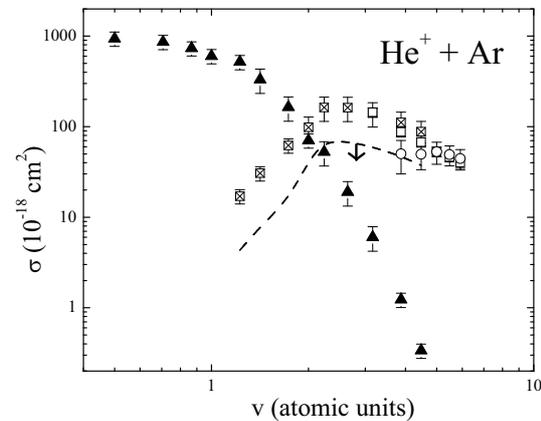

FIG. 2: Projectile charge-changing cross sections for $He^+ + Ar$ collisions. Triangles: electron capture [14]. Squares: projectile electron-loss with target ionization (Solid squares from Ref. [17] and open squares from Ref. [14]). Circles: projectile electron loss without target ionization (obtained combining data from Refs. [17] and [19]). The dashed line is an estimate for the upper bound for *screening* projectile electron loss from Ref. [14].

that found, for instance, in the $He^+ + Ar$ collisions (see Fig. 2). Two suggestions are offered to explain this behavior. One possibility is the absence of the electron capture collision channel for the anion projectile, since there is no stable doubly-charged atomic anion. The coupling between electron capture and other collision channels could, thus, be fundamental for positive low velocity projectiles and absent for negative projectiles. Another point to be considered is the high asymmetry in the projectile and target binding energies for $F^- + Ar$ collisions. This may result in a higher probability to lose a projectile electron without ionizing the target in the case of negative projectiles.
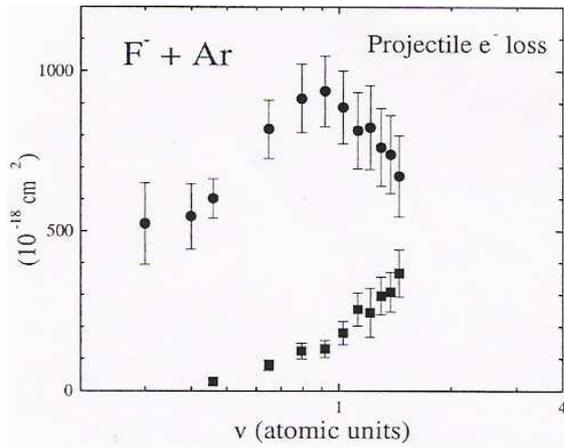
FIG. 3: Projectile electron-loss cross sections (single + multiple) as a function of projectile velocity for $F^- + Ar$ collisions. Squares, loss with target ionization [16]: $F^- + Ar \rightarrow \sum_{p>-1} F^{p+} + \sum_{q>0} Ar^{q+}$. Circles, loss without target ionization (obtained combining data from Refs. [16] and [7]): $F^- + Ar \rightarrow \sum_{p>-1} F^{p+} + Ar^0$.
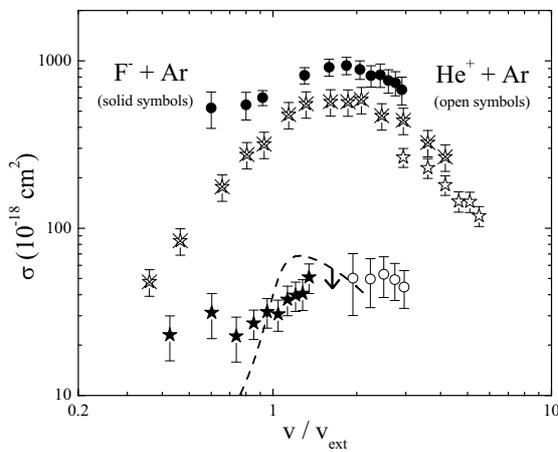

FIG. 4: Cross sections for the $F^- + Ar$ and $He^+ + Ar$ collision channels with no charge-changing of either target or projectile. (I) Solid symbols are used for $F^- + Ar$: stars, target total direct ionization [16]; $F^- + Ar \rightarrow F^- + \sum_{q>0} Ar^{q+}$; circles, projectile electron loss without target ionization (see Fig. 1). (II) Open symbols are used for $He^+ + Ar$: stars, target total direct ionization [20]; x-center stars, target direct ionization [14]; Circles (and dashed line), see Fig. 2.

Figure 4 highlights this asymmetry comparing projectile *screening* electron loss (the projectile elastic loss) and the target direct ionization, for both $F^- + Ar$ and $He^+ + Ar$ collision systems. Solid circles represent F^- electron loss without target ionization. Solid stars represent total target direct ionization for the F^- projectile. Open circles represent He^+ projectile electron loss without target ionization. Open and x-center stars represent total target direct ionization for the He^+ projectile. Cross sections are shown as a function of the projectile velocity divided by

$$v_{ext} = (I_{ejec}/Ry)^{1/2} \, v_0, \qquad (2)$$

where I_{ejec} is the first ionization potential (in Rydberg units) of the only collision partner (projectile or target) that has one or more ejected electrons. The parameter v_{ext} is a velocity characteristic of the *screening* electron loss and of the direct ionization process. It is equal to $0.500 \, v_0$ for F^-, $1.08 \, v_0$ for Ar, and $2.00 \, v_0$ for He^+. Cross sections are summed over contributions for final charge states q from 1 to 4 for Ar^{q+}, 0 to 2 for F^{q+}, and 1 to 2 for He^{q+}.

Projectile *screening* electron loss and target direct ionization are collision channels symmetric in the exchange of projectile and target frames of reference. With the projectile velocity parameterization used, $F^- + Ar$ *screening* electron loss and $He^+ + Ar$ direct ionization clearly show maxima at the same velocity region of Fig. 4. The two other collision channels presented in Fig. 4 are also consistent with maxima in the same velocity region but unfortunately the velocity range of available experimental data is too narrow to check this point.

Figure 4 shows *screening* electron loss much larger than target direct ionization in $F^- + Ar$ collisions, for which projectile binding energy (3.40 eV) is smaller than the target binding energy (15.8 eV). For $He^+ + Ar$ the situation is the opposite. The projectile binding energy (54.4 eV) is larger than the target binding energy (15.8 eV) and target direct ionization is much larger than projectile *screening* electron loss.

IV. SUMMARY

A comparison between projectile electron loss cross sections for negative, F^-, and positive, He^+, projectiles is presented for collisions with Ar target. The behavior of the two collision systems is similar for the projectile electron loss with target ionization (the *antiscreening* electron-loss process).

For projectile electron loss without target ionization (basically the *screening* electron-loss process), quite different situations are presented for the studied positive and negative projectiles. For $He^+ + Ar$, the loss without target ionization collision channel is negligible for intermediate-to-low energies. For $F^- + Ar$, this collision channel is the dominant in the total projectile electron loss at intermediate-to-low velocities. These different behaviors for positive and negative projectiles can be understood, at least in broad lines, considering two points: (I) coupling with the capture collision channel does not exist for negative projectiles; and (II) projectile binding energies are much smaller for the projectile than for the target in the case of anion-atom collisions. For cation-atom collisions the situation is usually the opposite one with binding energies higher for the projectile than for the atomic target.

[1] T. Kirchner, A. C. F. Santos, H. Luna, M. M. Sant'Anna,W. S. Melo, A. C. F. Santos, G. M. Sigaud, and E. C. Montenegro, Phys. Rev. A **72** 012707 (2005).

[2] V. Shevelko and H. Tawara 1998 in Atomic multielectron processes (Springer-Verlag).

[3] F. Zappa, A. L. F. de Barros, L. F. S. Coelho, Ginette Jalbert, S. D. Magalhães, and N. V. de Castro Faria, Phys. Rev. A **70**, 034701 (2004).

[4] J. H. Mcguire 1997 in Electron correlation dynamics in atomic collisions (Cambridge University Press).

[5] E. C. Montenegro, J. H. Mcguire and W. E. Meyerhof, Adv. At. Mol. Opt. Phys. **29** 217 (1992).

[6] M. M. Sant'Anna, F. Zappa, A. C. F. Santos, A. L. F. Barros, W. Wolf, L. F. S. Coelho, and N. V. de Castro Faria, Plasma Phys. Control. Fusion **46**, 1009 (2004).

[7] F. Zappa, Ginette Jalbert, L. F. S. Coelho, A. B. Rocha, S. D. Magalhães, and N. V. de Castro Faria, Phys. Rev. A **69**, 012703 (2004).

[8] F. Zappa, L. F. S. Coelho, G. Jalbert, A. B. Rocha, S. D. Maga-lhaes, and N. V. de Castro Faria, Braz. J. Phys. **34**, 825 (2004).

[9] E. C. Montenegro, W. S. Melo, W. E. Meyerhof and A. G. de Pinho, Phys. Rev. Lett. **69**, 3033 (1992).

[10] E. C. Montenegro, W. S. Melo, W. E. Meyerhof and A. G. de Pinho, Phys. Rev. A **48**, 4259 (1993).

[11] R. Dörner, V. Mergel, R. Ali, U. Buck, C. L. Cocke, K. Froshauer, O. Jagutzki, S. Lencinas, W. E. Meyerhof, S. Nüttgens, R. E. Olson, H. Schmidt-Böcking, L. Spilberger, K. Tökesi, J. Ulrich, M. Unverzagt, and W. Wu, Phys. Rev. Lett. **72**, 3166 (1994).

[12] H. Kollmus, R. Moshammer, R. E. Olson, S. Hagmann, M. Schulz, and J. Ullrich, Phys. Rev. Lett. **88**, 103202 (2002).

[13] G. M. Sigaud, and E. C. Montenegro, Braz. J. Phys. **33**, 382 (2003).

[14] R. D. DuBois, Phys. Rev. A **39**, 4440 (1989).

[15] W. S. Melo, M. M. Sant'Anna, A. C. F. Santos, G. M. Sigaud, and E. C. Montenegro, Phys. Rev. A **60**, 1124 (1999).

[16] M. M. Sant'Anna, F. Zappa, A. C. F. Santos, A. L. F. Barros, W. Wolf, L. F. S. Coelho and N. V de Castro Faria, (to be published).

[17] E. C. Montenegro, A. C. F. Santos, W. S. Melo, M. M. Sant'Anna, and G. M. Sigaud, Phys. Rev. Lett. **88**, 013201 (2002).

[18] A. C. F. Santos *et al.*, to be published.

[19] M. M. Sant'Anna, W. S. Melo, A. C. F. Santos, G. M. Sigaud, and E. C. Montenegro, Nucl. Intrum. Methods B **99**, 46 (1995).

[20] A. C. F. Santos, W. S. Melo, M. M. Sant'Anna, G. M. Sigaud, and E. C. Montenegro, Phys. Rev. A, **63**, 062717 (2001).